4-30-2002

Comparision of Measured Convection Velocities With Calcuulations Based On Electric Potential Model

Daniel E. Britton

Honors Senior Project
Proposal

Form 1 - Submitted at beginning of project proposal as soon as student and advisor set on project.

Proposed Title: Comparison of Measured Convection Velocities with Calculations Based on an Electric Potential Model

Name: Daniel E. Britton

Address: 2330 Little Cove Rd
(Street)

Hampton Cove AL 35763
(City) (State) (Zip)

Proposal approved by:

Project Advisor: [signature] Date: May 2, 2002

Department Chair: [signature] Date: 2 May 2002

Received in Honors Office: 5/2/02
(date)

Approved by Honors Council: 5/7/02
(date)

Signature of Honors Program Director: [signature]

Honors Senior Project
Approval

Form 3 – Submit with completed thesis. All signatures must be obtained.

Name of candidate: Daniel E. Britton

Department: Physics

Degree: Physics

Full title of project: Comparison of Measured Convection Velocities with Calculations Based on an Electric Potential Model

Approved by:

[signature] May 2, 2002
Project Advisor Date

[signature] 2 May 2002
Department Chair Date

Honors Program Director for Honors Council Date

The University of Alabama in Huntsville

Comparison of Measured Convection Velocities with Calculations Based on an Electric Potential Model

A Report for the Course
PH-499 Physics Practicum
with Dr. J. L. Horwitz

By
Daniel E. Britton

April 30, 2002

Abstract. A software model used to compute electric potentials in the ionosphere has been obtained and its output compared with ion convection velocities as measured by the TIDE spacecraft. The velocity measurements were obtained at an altitude of approximately 5000 kilometers over the southern ionosphere. Previous studies yield a high level of confidence in the TIDE measurements. To an adequate level of precision, the model's output correlates well with the TIDE velocity data.

Introduction

When the solar wind and its embedded interplanetary magnetic field (IMF) encounters the earth's magnetic field, complex interactions occur that lead to the generation of electric fields in the high-latitude ionosphere [*Weimer*, 1996]. Much work has been devoted to mapping these electric fields and the associated plasma convection vectors, encompassing both theoretical and empirical models, by *Heppner* [1972], *Heelis et al.* [1982], *Foster* [1983], *Heppner and Maynard* [1987], *Rich and Hairston* [1994], *Shue* and *Weimer* [1994], and *Papitashvili et* al, [1994]. These early maps indicated a need for a flexible numerical model [*Weimer*, 1996]. One model was developed in 1996 by D. R. Weimer of Mission Research Corporation using a technique for least error fit of empirical data collected by various earth-orbiting satellites [*Weimer*, 1996]. Having large quantities of data measured by other spacecraft available for comparative analysis, our goal was to determine the suitability of the model. Since the model requires empirically determined parameters as input, we were able to use data from one set of satellites to parameterize the model while using data from other satellites for comparisons.

In this report, we used sets of data obtained from the IMP-8 spacecraft. The satellite was launched by NASA on October 26, 1973 into a northern hemisphere elliptical orbit with an apogee of 45 R_E geocentric distance and a perigee of 25 R_E. Its purpose was to measure the magnetic fields, plasmas, and energetic charged particles of the near-earth solar wind. Additionally, ion drift velocities were obtained from the Thermal Ion Dynamics Experiment (TIDE) as measured by two POLAR spacecraft. The POLAR craft were launched in February 1996 into an near circular polar orbit with an apogee of 9 R_E geocentric distance, a perigee of 1.8 R_E, and an altitude of 840 km in the northern hemisphere, orbiting within 30 minutes or less of each other. The satellites measure ion drifts, densities, and temperatures in the topside ionosphere [*Zeng et al.*, 2001].

Technique

It can be shown that the drift velocity of moving particles in the ionosphere is proportional to the cross product of the electric field and the magnetic field, and is therefore perpendicular to both:

$$\vec{v} = \frac{\vec{E} \times \vec{B}}{B^2} \tag{1}$$

[*Kivelson and Russell*, 1995, p. 31]. The derivation is straightforward, and can be found in Appendix B.

The model we used can compute the electric potential at any point given a set of parameters describing the IMF [*Weimer*, 1996]. The output of these models can be graphed as contour plots, in which the gradient of the plotted potentials will be electric field lines perpendicular to the electric potential contour lines. This is because each contour line represents constant potential; as it compares to a nearby contour line, the gradient of the potential will be the orthogonal change between the two lines. By equation (1), the convection velocity is proportional to the cross product of the **E** and **B** fields; thus, it will be perpendicular to both. In a plot of the velocities alongside the contour lines, assuming **B** is orthogonal to the plane in which lies the contour line, at each point on the contour line the convection velocity vector should be tangential to the contour line. Then the two vector quantities, **E** and **v**, should be perpendicular to each other. In this way, we can graphically compare ion convection velocities to the electric potential to confirm our predictions. Additionally, we can numerically compute **E** and we have **v** from the empirical TIDE data. The calculated angle between **E** and **v** should be 90 degrees.

Having established the predicted orthogonality of direction of the **E** and **v** vectors, we can perform a further comparison by considering the magnitude of the vectors. From equation (1), we should be able to compare the magnitude of the velocity vector with the magnitude of $E \times \mathbf{B} / B^2$.

Data Analysis

In 1996, D. R. Weimer of Mission Research Corporation developed a new technique for forming an equation describing the electric potential at points in the ionosphere. The technique used least error fit of empirical data collected by various earth-orbiting satellites to determine the coefficients of a known equation [*Weimer*, 1996]. Dr. Weimer subsequently developed a FORTRAN software implementation of this model, and later released an improved version. Dr. Weimer graciously provided us with a copy of his software for use in this project.

The Weimer modeling software requires several inputs in order to compute an electric potential. The inputs are:

- IMF Y-Z Clock Angle
  The IMF clock angle is measured in degrees, where zero indicates north and 180 degrees indicates south. It is calculated from the *y* and *z* components of the IMF and is given by *arctan(y/z)*.
- Magnitude of IMF in Y-Z plane
  This value is expected to be given in nanoTesla (nT).
- Dipole Tilt Angle
  Measured in degrees, the dipole tilt angle measures the angle between the earth's rotational north pole and its magnetic north pole.
- Solar Wind Velocity (Magnitude)
  Measured in km/s, this is simply the magnitude of the solar wind velocity vector.
- Solar Wind Density
  The solar wind density is a measurement of the count of ions per unit volume. The solar wind is dominated by hydrogen nuclei; therefore, the density is a

measure of protons per unit volume. The Weimer software expects this quantity in counts per cubic centimeter.

- Latitude

  The latitude of interest, measured in the AACGM coordinate system.

- Magnetic Local Time

  The magnetic longitude of the observer minus the magnetic longitude of the sun expressed in hours plus 12.

We obtained empirical data for input into the model for the period 12:22 – 12:53 UT May 27, 1996. IMP-8 provided data to determine IMF Y-Z clock angle, IMF magnitude, and solar wind velocity and density, while dipole tilt angle and ion flow velocities were obtained from TIDE data. Because the Weimer model works exclusively in Altitude Adjusted Corrected Geomagnetic Coordinates (AACGM) coordinates, transformations were required.

Understanding the AACGM system first requires an understanding of the geomagnetic coordinate system (MAG). In the MAG system, the *x*-axis points toward the sun, the *z*-axis is parallel to the earth's magnetic axis, and the *y*-axis is perpendicular to the geographic poles. This system is convenient for tracing magnetic field lines. The magnetic longitude is measured eastward from the *x*-axis, and magnetic latitude is measured from the equator in magnetic meridians, positive when measuring northward [*Kivelson and Russell*, 1995, p 533-4]. CGM, the Corrected Geomagnetic Coordinate System, was introduced to express data points in terms of the true geomagnetic field. Indeed, the CGM system accounts for differences in altitude. However, in the AACGM system, points at nonzero altitudes are projected onto the surface of the earth to determine the magnetic latitude. The result is that in the AACGM system, any two points connected by a magnetic field line will have the same magnetic latitude and longitude regardless of altitude. The same is true in the CGM system only at zero altitude.

Every data source required a coordinate transformation before it could be used with the Weimer software. Furthermore, some of the data required interpolation to fit the sampling times of the initial data set. The source data were in several different text files of varying formats, so we chose the Perl programming language since it is well suited to text manipulation to extract the data points and merge them into a single input file. For simplicity, several Perl programs were written to convert the inputs in steps.

Unfortunately, while the TIDE and IMP-8 data were gathered in orbit over the southern hemisphere, the Weimer model was only designed to work in the northern hemisphere. However, with modifications to the input data suggested by Dr. Weimer, accurate values for the southern latitudes could be obtained with the model. In particular, the model requires the absolute values of the latitudes, and that the dipole tilt angle and the IMF y coordinate used in calculating the clock angle be negated. To verify that the modifications resulted in a reasonable model for the southern latitudes, we first ran the model with the same parameters used by Dr. Weimer in his original paper [*Weimer*, 1996]. We then altered the parameters to produce a corresponding map of the southern hemisphere. If the model worked correctly, the contour plots should show symmetry. Regrettably, the outputs failed to show any unquestionably discernable symmetry (see Fig 4a and 4b in Appendix A). Regardless, we assumed the model was correct in the gross sense (symmetry indicates that the southern potentials should be much the same as the northern potentials) and pressed on.

We modified the output of the Weimer model to be in a cylindrical coordinate system in which r, θ, z represent latitude, magnetic local time (MLT), and z is along the magnetic pole as in the AACGM system. (We henceforth refer to this modified cylindrical system as MLT.) In our plots, latitude ranges from 90° (at the pole) to approximately 45.5°, and instead of plotting angular values from zero to 2π, θ ranges from zero to 24 hours. Onto this plot, we overlaid the POLAR satellite's trajectory and discrete vectors indicating the ion drift velocity at the times of measurement.

As the ions approach earth, their trajectories are nearly parallel. When an ion comes under the influence of earth's magnetic field, it falls toward the pole along a magnetic field line, which is curved. Near perigee at 5000 km altitude over the southern polar region, the particle's trajectory is somewhat parallel to the ecliptic plane. However, the modified Weimer model yielded electric potentials valid only near the earth's surface (approximately 100 km). In order to compare ion convection velocities with velocities calculated from these potentials, we needed to consider how the velocity vector would change as the particle fell along the curved field line toward the surface of the earth.

The velocity vector data used a magnetic local coordinate system. That is, the axes of the Cartesian system are oriented with *x* toward the sun, *y* toward dusk, and *z* oriented with the magnetic pole. When considering convection velocities, we are only interested in the *x* and *y* components of the velocity vector. Since each curved field line lies in a single vertical plane, and each such plane is coplanar with the magnetic local *z* axis, we made the assumption that the components of the velocity vectors – the *x* and *y* coordinates – in which we were interested would not change significantly.

We focused on a set of data obtained for the time period 12:22 – 12:53 UT May 27, 1996. Once a contour plot of the electric field was produced using the Weimer model for this period, an overlay plot of the satellite positions for each discrete data point was constructed from corresponding TIDE data. The IDL plotting routines used worked exclusively in Cartesian coordinates; therefore, using IDL we converted the cylindrical coordinates output from the Weimer model to Cartesian. The IDL Cartesian system was oriented such that the *x*-axis was to the right, the *y*-axis up, and the *z*-axis coming out of the paper. On the other hand, the satellite tracking position data were given in GSM coordinates. In this system, which has its origin at the center of the earth, the *x*-axis points from the earth to the sun, and the *y*-axis lies in the ecliptic plane and points toward dusk (opposite the earth's direction of revolution about the sun). The *z*-axis then is the same as the north magnetic pole. This was an ideal provision for overlaying on the MLT plot.

For each data point indicating the satellite position, we also had vector components for the total ion velocity. Using an existing program, we were able to extract the convection velocity part of the total ion velocity. The ion velocity is comprised of a component parallel to the magnetic field line, which we ignored. The other part of the velocity is the convection velocity, which is perpendicular to that same field line. The velocities are provided in the GSM system; as such, we assumed that we could safely ignore the *z* component of the velocity, because that would be the entire perpendicular velocity constituent in which we have no interest. The program we used incorporates exotic criteria such as the spin of the spacecraft; however, it ignores trivial effects such as the influence of precession on the planarity of the satellite's polar orbit. The output of this program was not the *x* and *y* components of the convection velocity vector; instead, it was a simpler quantity, the angle formed between the satellite's direction of travel and the *x-y* direction of the ions' velocities. We could then easily plot this invariant quantity corresponding to the predicted conditions near earth's surface.

Figure 1 in Appendix A shows the entire South Magnetic Pole region. The Weimer model provided electric potential values, which are graphed as contour lines. Onto the contour plots, we overlaid the track of the satellite. The convection velocities were then plotted as another overlay, with the origin of each vector being the position of the satellite when a data point was recorded. We plotted the magnitudes of the recorded convection velocities, although in this particular comparison, we were only interested in direction. We chose a reasonable, constant magnitude for the vectors for clarity. From the earlier discussion, we know that these ion convection velocities should be tangential to the contour lines; however, this is difficult to distinguish from the dense plots in Figure 1.

Figure 2 provides a close-up view of the beginning of the satellite data set. As before, the vectors originate from the satellite's path; however, we omitted the satellite path for clarity. From this close-up plot, it is apparent that the velocity vectors are indeed tangential to the contour lines. Figure 3 provides another close-up view of a different part of the satellite path and associated data. This view also illustrates the approximate tangential relationship.

While plots of this data give a qualitative sense of the relationship between the convection velocities and the contour lines, the orthogonal relationship between the gradient and the drift velocity is not convincingly clear. Numerical computations are required to fully establish the relationship. To perform the comparison, we required the field gradient vectors themselves. We calculated these by the following method, illustrated in Diag. 1 and 2: Take any three nearby points and use the Weimer model to calculate the electric potential at each. Form two vectors between the three points, such that the tails of the vectors coincide at one of the points. Using the Cartesian coordinates for these vector endpoints, normalize these unit vectors, removing the units of length. Appropriately multiply the difference in the electric potential values at these points. The vector sum of these two vectors will give the electric field vector. This vector can then be compared to the ion drift velocity vectors to verify orthogonality.

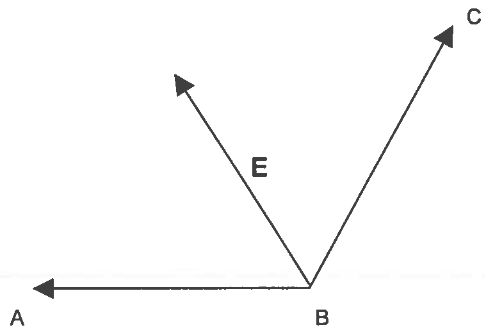

Diag 1: Computing electric field vector **E**. *The Weimer model yields potentials at points A, B, and C; the vector sum is used to obtain the gradient vector* **E**.

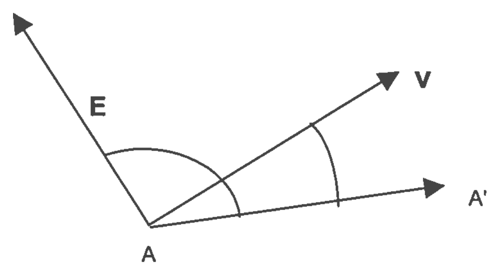

Diag 2: Verifying orthogonality. The satellite moves from point A to point A′. The angle between the satellite path and the convection velocity is known; that between the path and the electric field vector **E** *can be calculated.*

When this method was applied to the data under consideration, the average calculated value for the angle between **E** and **v** was 71.2 degrees (see Fig 5 in Appendix A), albeit with a high degree of deviation: 60.6 degrees.

In a final comparison, we calculated the magnitude of the E-cross-B drift velocity using electric field vectors obtained from the previous step with IMP-8 measurements of the magnetic field vectors. We then plotted these calculated magnitudes and the measured TIDE velocities at the same points in time (see Fig 6 in Appendix A). The average error was only 16 %, although as with the computed angles, there was a high deviation in the calculated magnitudes.

Conclusion

To a good approximation, our graphical analysis shows that the Weimer model output does indeed correlate with empirical data. The model's appropriateness is further reinforced by numerically analyzing the available data to determine orthogonality, which was shown to within 20% error. Not only did we compare directions of these vectors; we were further able to compare the magnitude of the convection velocity with the magnitude of the **E** and **B** fields according to equation (1), with a resulting error of 16%. As in the previous analyses, the model proves satisfactory on a gross scale.

In a future refinement of this work, we suggest incorporating a program that performs magnetic field line tracing. For a satellite at altitude (approximately 5000 km), the tracing program can accurately alter the vector quantities measured by the satellite as if they were measured directly on the earth's surface (an obvious impossibility). Using the tracing program, we could validate our assumption that the *x-y* components of the convection velocity vectors do not vary significantly with altitude. Furthermore, there were odd variations in the measured velocity vectors as well as the failure to obtain symmetric plots for both northern and southern latitudes that could point to a failure of the Weimer model to accurately model the southern latitudes. In aggregate, however, our comparisons show that the model is fairly good.

Acknowledgements. The author acknowledges CDAWeb for the use of online IMP-8 data, NASA's Marshall Space Flight Center for online access to TIDE data, and SuperDARN for coordinate transformation software routines. The author also wishes to thank Mr. J.-N. Tu for his ideas and methodologies which formed the basis of this report.

References

Chen, Francis F., 1984. Introduction to Plasma Physics and Controlled Fusion. New York: Plenum Press.

Foster, J. C., An empirical electric field model derived from Chatanika radar data, *J. Geophys. Res., 88*, 881-987, 1983.

Hairston, M. R., and R. A. Heelis, Model of the high-latitude ionospheric convection pattern during southward interplanetary magnetic field using DE 2 data, *J. Geophys. Res., 95*, 2333-2343, 1990.

Heelis, R. A., J. K. Lowell, and R. W. Spiro, A model of the high-latitude ionospheric convection pattern, *J. Geophys. Res., 87*, 6339-6345, 1982.

Heppner, J. P., Polar cap electric field distribution related to the interplanetary magnetic field direction, *J. Geophys. Res., 77*, 4877-4887, 1972.

Heppner, J. P. and N. C. Maynard, Empirical high-latitude electric field models, *J. Geophys. Res., 92*, 4467-4489, 1987.

Khazanov, G. V., C. E. Rasmussen, Yu. V. Konikov, T. I. Gombosi, and A. F. Nagy, Effect of magnetospheric convection on thermal plasma in the inner magnetosphere, *J. Geophys. Res., 99,* 5923-34, 1994.

Kivelson , Margaret G. and Christopher T. Russell, ed 1995. Introduction to Space Physics. New York: Cambridge University Press.

Papitashvili, V. O., B. A. Belov, D. S. Faermark, Ya. I. Feldstein, S. A. Golyshev, L. I. Gromova, and A. E. Levitin, Electric potential patterns in the northern and southern polar regions parameterized by the interplanetary magnetic field, *J. Geophys. Res., 99*, 12,251-13,262, 1994.

Rich, F. J., and N. C. Maynard, Consequences of using simple analytical functions for the high-latitude convection electric field, *J. Geophys. Res., 94*, 3687-3701, 1989.

Shue, J.-H., and D. R. Weimer, The relationship between ionospheric convection and magnetic activity, *J. Geophys. Res., 99*, 401-415, 1994.

Weimer, D. R., A flexible, IMF dependent model of high-latitude electric potentials having "space weather" applications, *Geophys. Res. Letters., 23*, 18, 2549-52, 1996.

Zeng, W., J. L. Horwitz, B. A. Stevenson, X.-Y. Wu, Y.-J. Su, P. D. Craven, F. J. Rich, T. E. Moore, and J.-N. Tu, Near-simultaneous Polar and DMSP measurements of topside ionospheric field-aligned flows at high latitudes, *J. Geophys. Res., 106*, 29, 601-29, 2001.

Appendix A

Fig. 1. Projection of convection velocity vectors with electric potential contour lines. Although not readily apparent at this scale, the vectors should be tangential to the contour lines. The satellite's path is from lower-left to upper-right.

Fig. 2. A close-up of part of the previous image. Note the apparent tangential nature of the convection velocity vectors.

Fig. 3. A close-up of another part of the plot. Quantitatively, the convection velocities appear reasonably tangential to the electric potential contour lines.

Fig. 4a. Weimer model for northern latitudes.

Fig. 4b. Weimer model modified to work for southern latitudes.

Fig 5. Calculated **E-v** angle. As compared to the expected value of 90 degrees, the average error is 20%.

Fig 6. Calculated E-cross-B drift velocity and empirical TIDE data. The average error is only 16%.

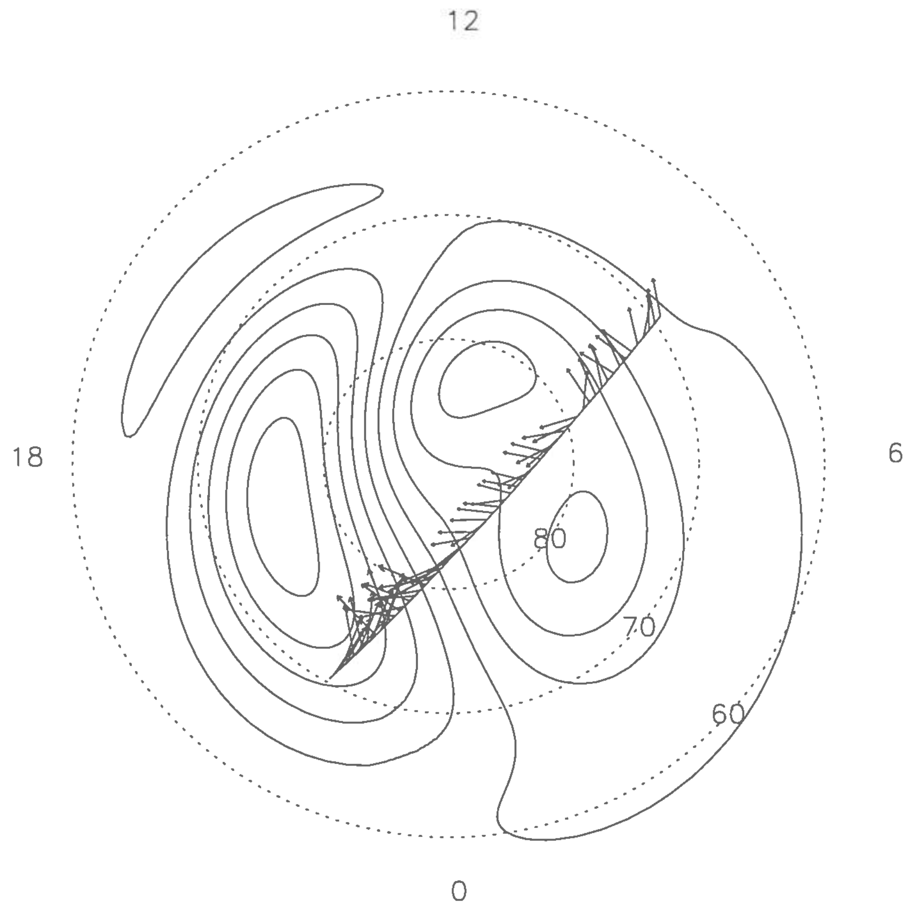

Fig. 1. Projection of convection velocity vectors over electric potential contur lines. Although not readily apparent at this scale, the vectors should be tangential to the countour lines. The satellite path is from lower–left to upper–right.

Data Set: 5/27/1996

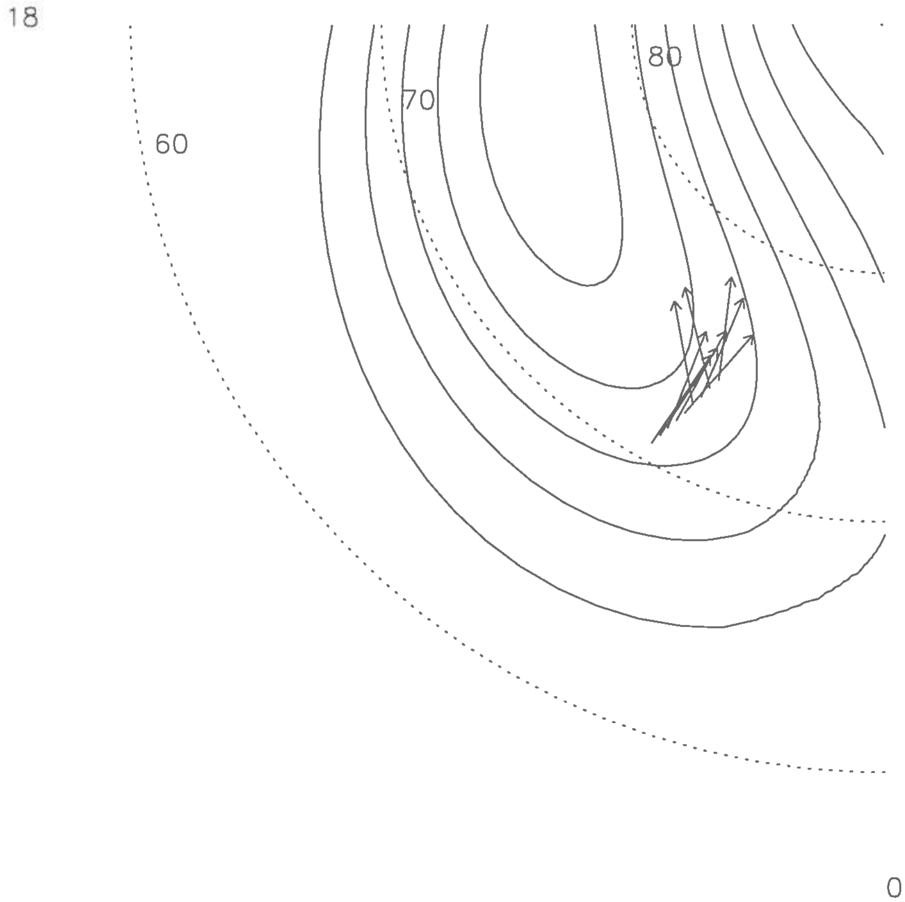

Fig. 2. A closeup of part of Figure 1. The convection velocity vectors appear to be tangent to the potential contours.

Data Set: 5/27/1996

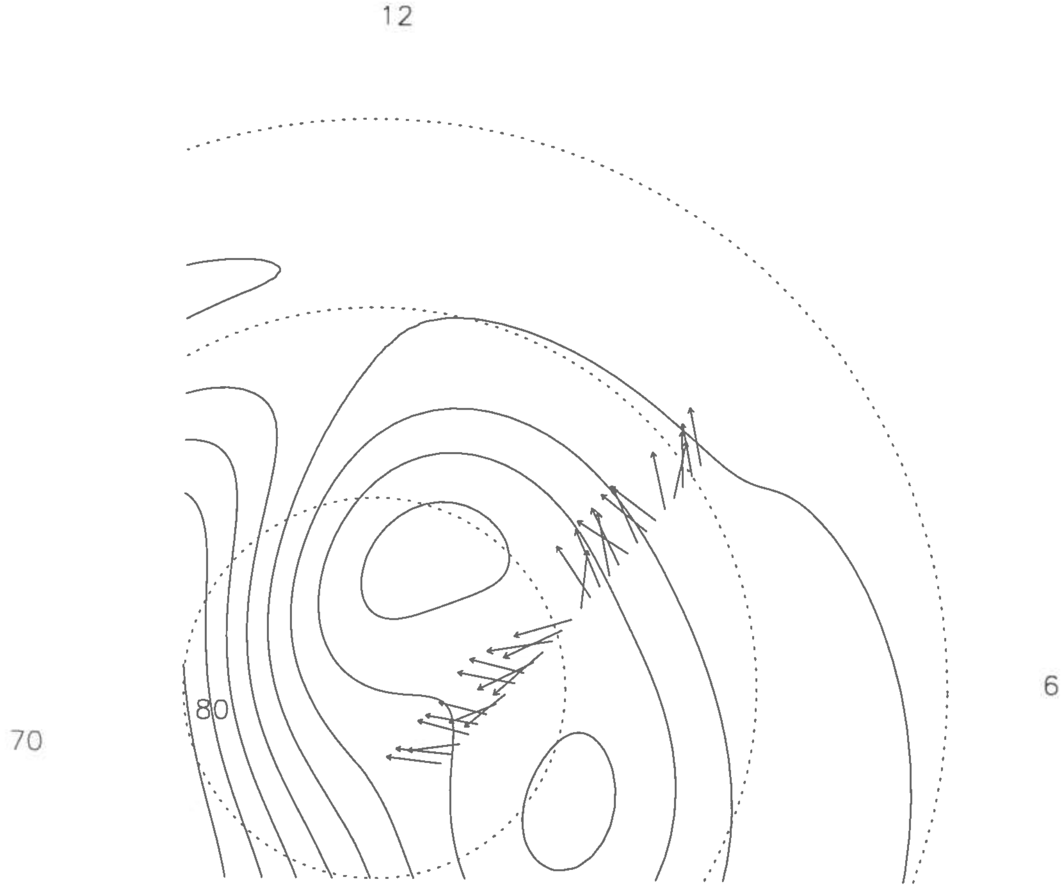

Fig. 3. A closeup of another part of Figure 1. Quantitatively, the convection velocities appear reasonably tangential to the electric potential contour lines, as expected.

Data Set: 5/27/1996

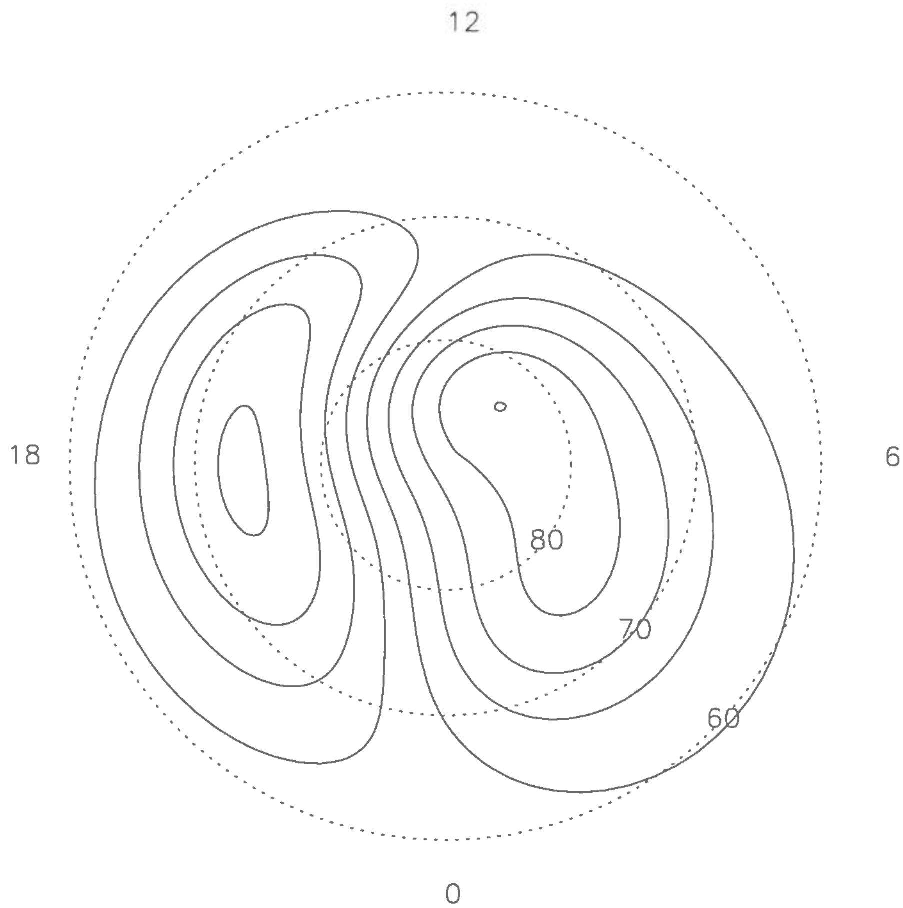

Fig. 4a. Weimer model for northern latitudes.

Data Set: Bt=10.0 nT, Tilt=0.0, Vsw=500 km/s, clock angle=−90.0 deg

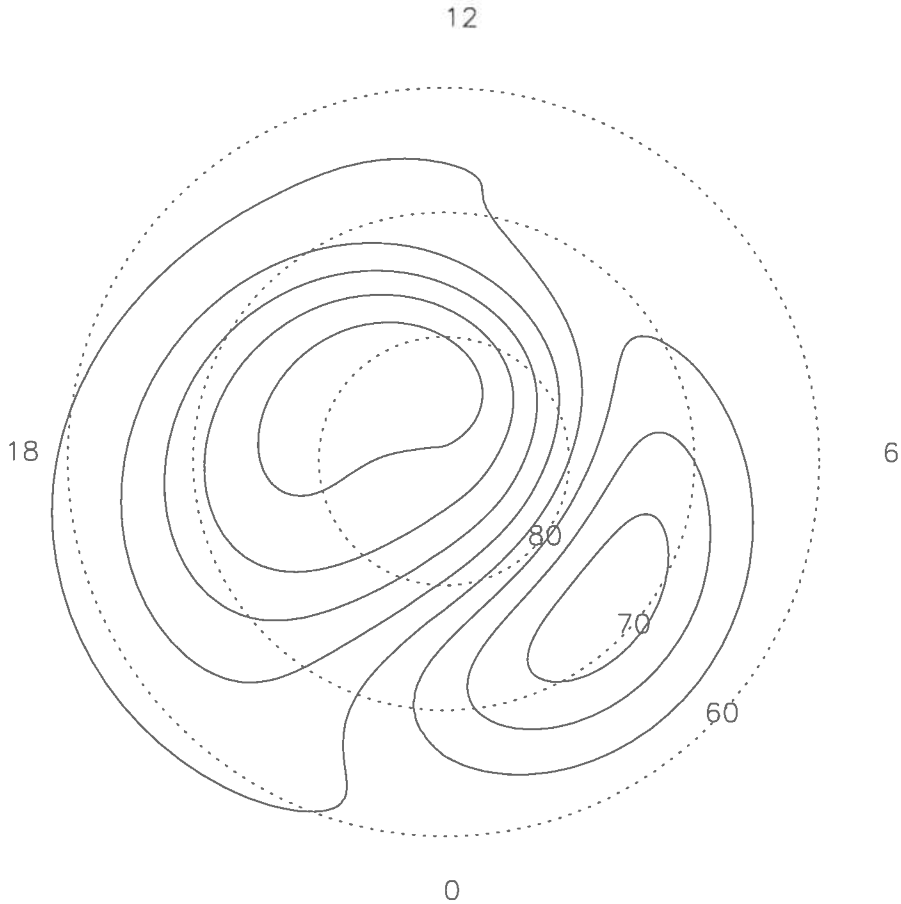

Fig. 4b. Weimer model modified to work for southern latitudes.

Data Set: Bt=10.0 nT, Tilt=0.0, Vsw=500 km/s, clock angle=90.0 deg

Fig 5. Calculated E-v Angle

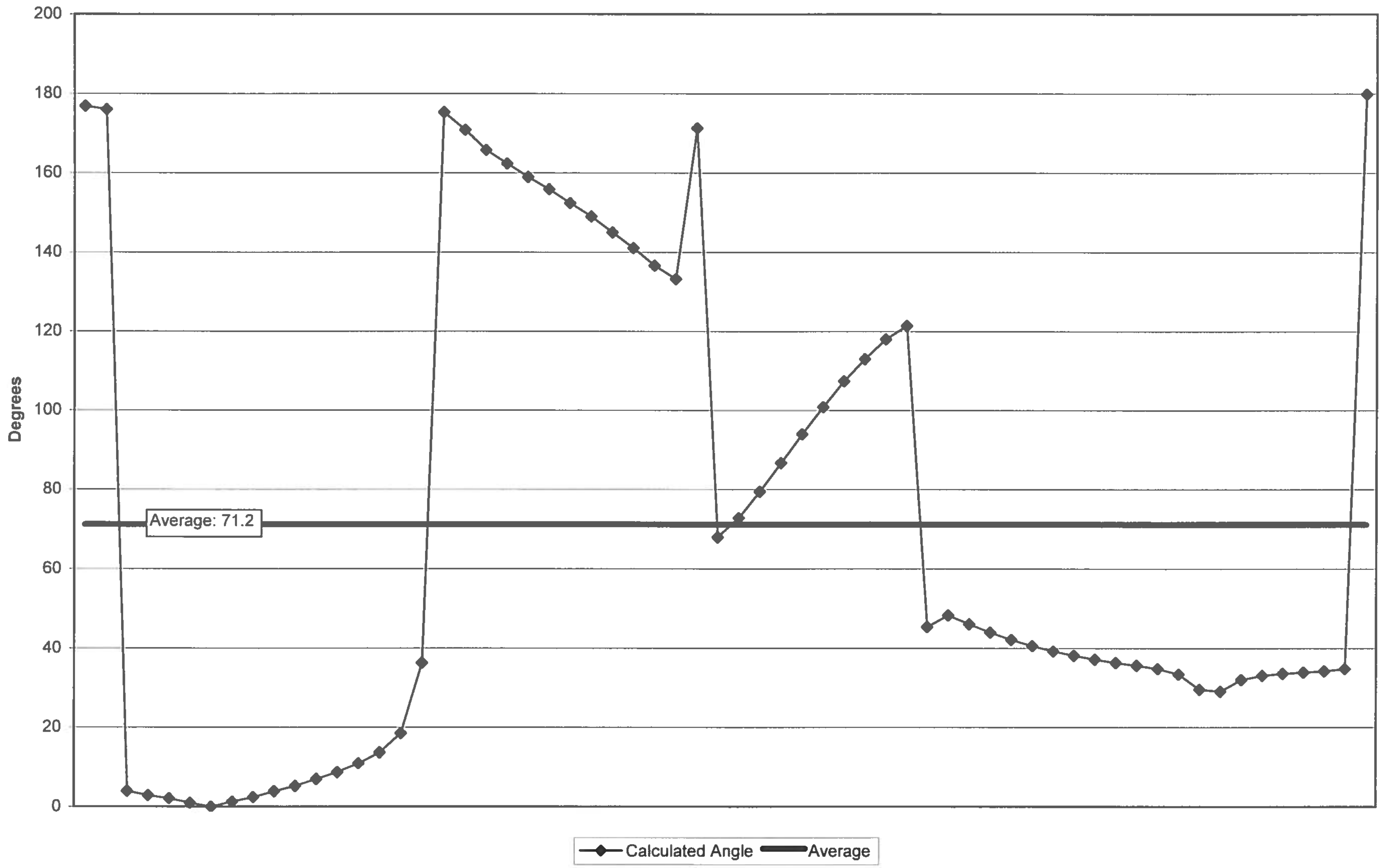

Fig 6. Velocity Comparison

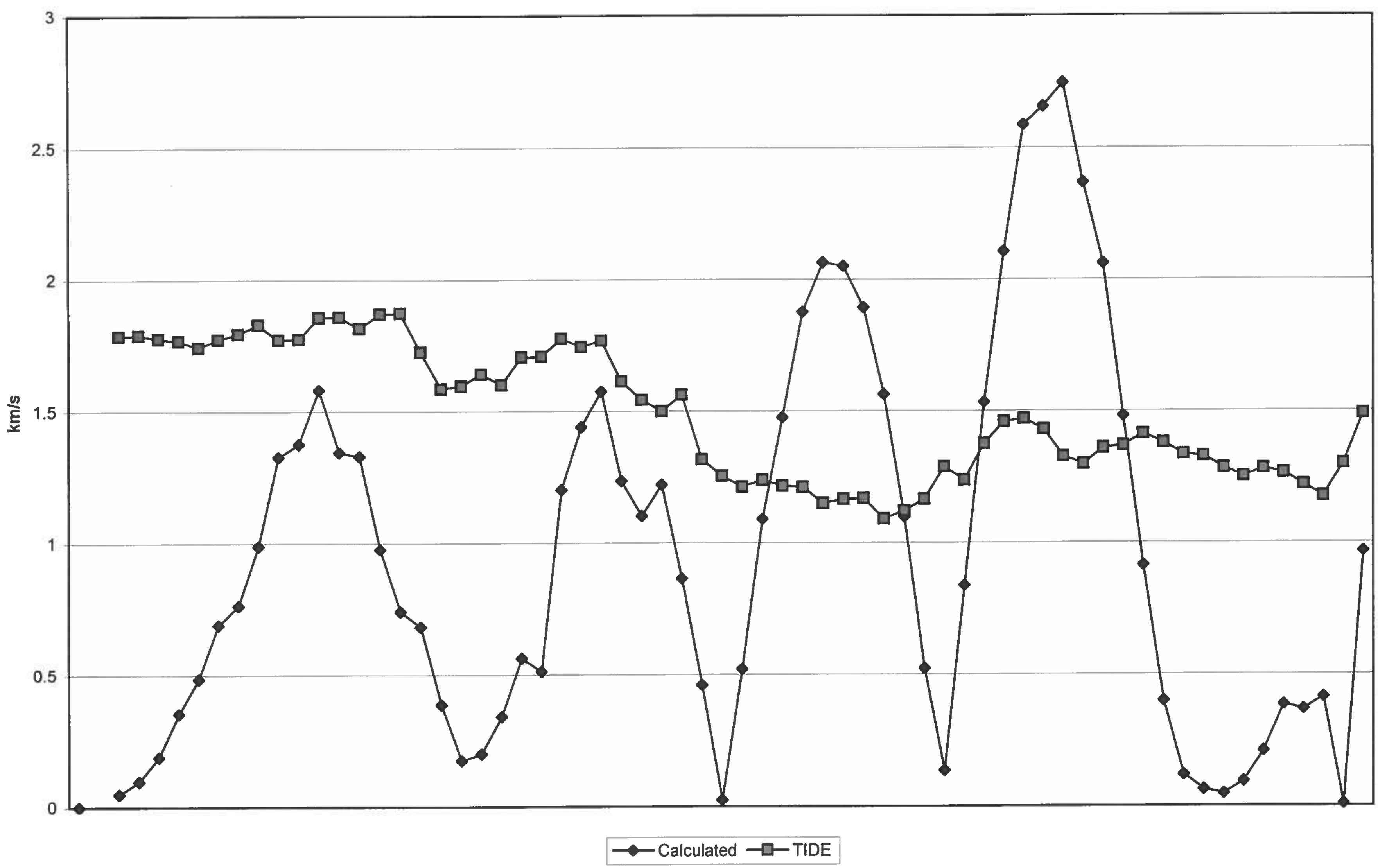

Appendix B
Derivation of E-cross-B Drift Velocity Equation

The drift-velocity equation is used throughout this report:

$$\bar{v} = \frac{\bar{E} \times \bar{B}}{B^2} \qquad (1)$$

We start with the Lorentz force equation in SI units:

$$\bar{F} = q\bar{E} + q\bar{v} \times \bar{B} \qquad (2)$$

From Newton's laws, for a particle of mass *m*, the rate of change of momentum (*m***v**) is expressed as:

$$m\frac{d\bar{v}}{dt} = q\bar{E} + q\bar{v} \times \bar{B} + \bar{F}_g \qquad (3)$$

$\mathbf{F_g}$ represents nonelectromagnetic forces, such as gravitation, which may be present. However, these forces are much smaller than other forces in the system, so we can set $\mathbf{F_g = 0}$ [*Kivelson and Russell,* 1995, p 28]. We can view the velocity as consisting of two parts: the gyroscopic velocity and the drift velocity [*Chen*, 1984, p 21-22]. Because the drift of the particle is assumed to be at constant velocity, the left hand side of the equation (3) is taken to be zero. [*Kivelson and Russell,* 1995, p 30].

$$\hat{0} = q(\bar{E} + \bar{v} \times \bar{B}) \qquad (4)$$

We can disregard the charge since the left hand side of (4) is zero:

$$\hat{0} = \bar{E} + \bar{v} \times \bar{B} \qquad (5)$$

Take the cross product of both sides with **B**:

$$\vec{B}\times\hat{0} = \vec{B}\times(\vec{E}+\vec{v}\times\vec{B}) \qquad (6)$$

Then by the cross product identity **a x (b+c) = a x b + a x c**:

$$\vec{B}\times\hat{0} = \vec{B}\times\vec{E}+\vec{B}\times(\vec{v}\times\vec{B}) \qquad (7)$$

But **a x (b x c) = (a · c) b – (a · b) c**:

$$\vec{B}\times\hat{0} = \vec{B}\times\vec{E}+(\vec{B}\bullet\vec{B})\vec{v}-(\vec{B}\bullet\vec{v})\vec{B} \qquad (8)$$

a · b = a b cos θ where θ is the angle between vectors **a** and **b**. If **b = a**, then **a · a** = a^2 cos θ and the angle is zero, so **a · a** = a^2, and equation (8) becomes:

$$\vec{B}\times\hat{0} = \vec{B}\times\vec{E}+B^2\vec{v}-(\vec{B}\bullet\vec{v})\vec{B} \qquad (9)$$

The drift velocity is perpendicular to the magnetic field [*Kivelson and Russell,* 1995, p 30]; thus, **B · v** = 0. Using the vector identity **a x b = -b x a**, and noting that **b x 0 = 0**:

$$\hat{0} = -\vec{E}\times\vec{B}+B^2\vec{v} \qquad (10)$$

Algebraic manipulation yields equation (1):

$$\vec{v} = \frac{\vec{E}\times\vec{B}}{B^2}$$